A Thermal Model of Drilling a Titanium Alloy (Ti-6Al-4V) Under Different Cooling Techniques

WCMNM 2021

Ankit Kumar[1], Rajneesh Bhardwaj[1] and Suhas S. Joshi[1]

[1]*Department of Mechanical Engineering, Indian Institute of Technology Bombay, Mumbai, 400076, India*

Abstract

Direct-injection of coolants in drilling reduces temperature, but heat dissipation does not happen positively. We developed two methods of cooling, such as Ti-Cu butt joint and heat sink based bottom channel cooling to improve heat dissipation. Numerical model of heat dissipation shows that temperature is reduced by 30 %, and 38 % in heat sink based cooling and Ti-Cu combination, respectively, in comparison to dry drilling. The numerically temperature lies within ~1-6 % of the experimental values.

Keywords: Drilling, Heat generation, Temperature distribution, Cooling, FEM

1. Introduction

The enclosed nature of a drilling process and lower thermal conductivity of titanium alloys [1], cause a layer of heat accumulation along the drill cutting edges during drilling. The resulting temperature influences tool life, surface roughness, and tool wear [2]. Direct-injection of coolants in drilling reduces temperature, but heat dissipation does not happen positively. In the past, Shakeel and Pradeep [3] found that using LN_2 as a coolant resulted in a 6-59% reduction in workpiece temperature. Suarez et al. [4] demonstrated a reduction in force and temperature in the nickel-based alloy when coolant is applied at a high pressure. Chowdhury et al. [5] found that flood cooling reduced tool temperature by 10% when compared to cold air mist cooling in a computational fluid dynamics (CFD) model. Using a CFD Model, Tahir et al. [6] discovered that cooling efficiency in the cutting process is affected not only by the input flow parameters, but also by the channel geometry of the tool. Salman et al. [7] present a coupled finite element method (FEM) and a CFD model that showed a significant reduction in tool temperature in flood cooling, as compared to air cooling. Patne et al. [8] used a FEM model that predicted nearly 50% increase in peak temperatures during drilling in the presence of tool wear.

We adopted new cooling techniques; such as Ti-Cu butt joint and a heat-sink based bottom channel cooling to improve heat dissipation during drilling of titanium alloy. The experimental temperature of the drill was measured by an infrared camera. At the same time, we used a numerical method to evaluate temperature distribution in a drill during drilling.

2. Experimental setup

A milling machine was used to conduct the experiments on drilling of titanium alloys under dry, Ti-Cu scheme, and bottom channel cooling, see Fig. 1(a). A dynamometer and infrared camera were used to record thrust, torque and temperature. The measured emissivity of the drill was found to be 0.36. To measure temperature of the drill more accurately, a thermal camera was positioned in-line with the axis of a small pin-hole of ϕ 2 mm that was drilled on the edge of the workpiece, as shown in Fig.1b. In the Ti-Cu combination, a higher thermal conductive material, such as copper was introduced as a heat dissipating material and was butt-jointed with Ti alloy using brazing, see Fig 1b. All holes are drilled at the interface of the materials. The Cu plate is expected to carry away the heat and reduce heat exposure to the cutting edges. In another method, bottom channel cooling device consisting of a plate channel made of copper was used for circulating the coolant. The workpiece to be drilled was glued to the channel such that it forms a top cover of the channel as shown in Fig 1c. As soon as the drill emerges out of the hole and

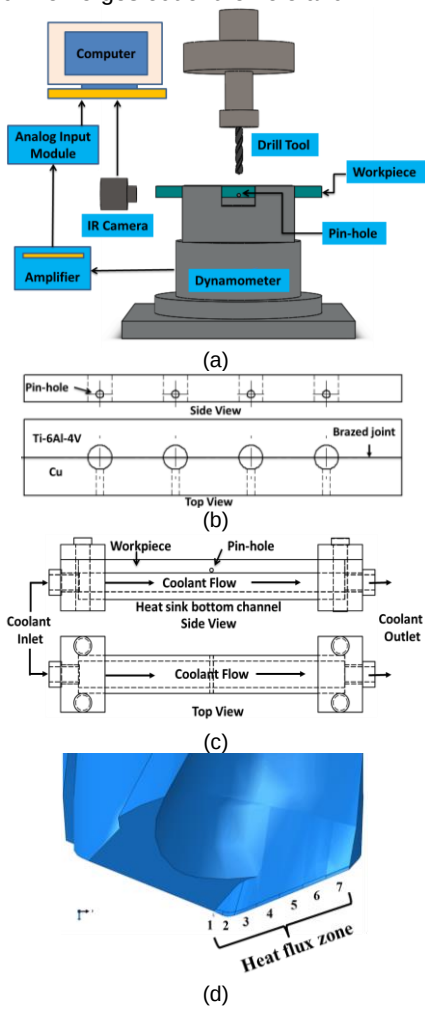

Fig. 1(a-d): (a) Schematic diagram of the experimental setup, (b) Schematic diagram of Ti-Cu scheme, (c) Schematic diagram of Bottom channel cooling (d) Elementary cutting tool (ECT) of drill cutting

into the channel, cooling water enters into the flutes of the drill. The coolant water flowing in the channel cools the workpiece along its bottom face, by effectively carrying away the heat generated during drilling, as it flows through the channel. Thus, the bottom cooling channel acts as a heat-sink.

3. Approach to modelling heat generation

Case (a): Heat generation in dry condition

The heat energy produced over the primary deformation zone is because of the material deformation in front of the cutting edge. The amount of heat gained by a tool while the chip moves on the tool rake face, and its partition factor (B_1) are related by [9]-

$$Q_{tool}^{shear} = (1-B_1)V_c\rho_w C_w T_s b a_c \quad (1)$$

$$B_1 = 1 + \frac{\pi}{2V_c \frac{a_c}{\alpha_w} \ln\left(\frac{2b}{l_c}\right)} \quad (2)$$

where, $T_s = T_0 + \Delta T_s$

$\Delta T_s = \frac{(1-\beta_w)F_s \cos\gamma}{\rho_w C_w a_o w \cos(\phi-\gamma)}$ (3), given by Oxley [10].

The frictional heat in the secondary region can be estimated by using experimentally evaluated thrust and torque using empirical correlations related to the machining process. The overall frictional heat generated due to flow of chip over the rake surface of a tool is given by [11][9] -

$$Q_{tool}^{friction} = B_2 Q_f = B_2 F_f V_c \quad (4)$$

$$B_2 = \left(1 + 0.45\frac{K_t}{K_w}\sqrt{\frac{\pi\alpha_w}{V_c l_c}}\right)^{-1} \quad (5)$$

The heat generated in the tertiary zone due to friction between the machined work surface and the flank face on the tool. The amount of heat generated along the tertiary zone, and its partition factor are given by [12][9] -

$$Q_{tool}^{flank} = (1-B_3)F_{cw}V \quad (6)$$

$$B_3 = \left(1 + \frac{\pi K_t}{2a_o V \ln(2b/V_b)}\right) \quad (7)$$

Case (b): Heat generation in Butt joint of Ti-Cu scheme

$$q_{\text{tool}} = (q_{\text{tool}}^{shear} + q_{\text{tool}}^{friction})_{Ti-alloy} + (q_{\text{tool}}^{shear} + q_{\text{tool}}^{friction})_{Cu} - q''_{\text{heat loss intersection}}$$

$$= \frac{1}{2}\left\{\begin{array}{l} \left(\frac{(1-B_1)V_c\rho_w C_w T_s b a_c}{l_c l} + \frac{B_2 Q_f}{l_c l}\right)_{Ti-alloy} \\ +\left(\frac{(1-B_1)V_c\rho_w C_w T_s b a_c}{l_c l} + \frac{B_2 Q_f}{l_c l}\right)_{Cu} \\ -2\frac{(T_{Ti-alloy} - T_{Cu})}{\left(\frac{l/2}{k_{Ti-alloy}}\right) + \left(\frac{l/2}{k_{Cu}}\right)} \end{array}\right\} \quad (8)$$

where, $T_{Ti-alloy} = T_0 + \Delta T_{Ti-alloy}$ and

$$\Delta T_{Ti-alloy} = \frac{\beta_w F_s \cos\gamma}{\rho_w C_w a_o w \cos(\phi-\gamma)} \quad (9)$$

Similary, ΔT_{cu} can be evaluated using Eq.(9).

This analysis is based on theoretical concepts by introducing a higher conductive material as close as possible to the Ti-alloy, which could increases cutting zone heat dissipation and improve tool life in a drilling process. The one half of the cutting edge involves heat generated in drilling by Ti alloy, and the second half of the cutting edge involves the heat generated by drilling copper. The average of heat flux applied on both materials is applied to individual ECTs and can be evaluated as in eq.(8).

Case (c): Heat Generation in Heat-Sink based Bottom Channel Cooling

The higher heat generated in drilling of Ti alloys can be reduced by the flow of water in the heat-sink along the bottom channel. The frictional heat was reduced by a reduction in thrust and torque force due to heat-sink based cooling. The heat is removed from the bottom of the workpiece by convection cooling. The overall heat generation on tool can be evaluated as –

$$q_{\text{tool}} = q_{\text{tool}}^{shear} + q_{\text{tool}}^{friction} - q_{\text{convection tool}} = \frac{(1-B_1)V_c\rho_w C_w T_s b a_c}{l_c l} + \frac{B_2 Q_f}{l_c l} - h(\mathrm{T} - \mathrm{T}_{room}) \quad (10)$$

where, V,V_c, ρ_w, C_w, α_w, K_w, β_w, K_t, T_o, b, a_c, a_o, F_s, F_f, l_c, l, γ *and* ϕ *are* cutting speed, Chip velocity, density, specific heat, Thermal diffusivity, thermal conductivity, Heat partition factor for workpiece, thermal conductivity of tool, room temperature, chip width, chip thickness, Uncut chip thickness, Shear force, friction force, contact length, elementary cutting length, rake angle and shear angle, respectively. T is assumed as maximum temperature in experimental work, and h is the convection heat transfer coefficient for water as given by [14]-

$$h = \frac{k_{water}}{x}(0.023\,\mathrm{Re}^{0.8}\,\mathrm{Pr}^{0.3}) \quad (11)$$

3.1 Formulation of FEM Model

The complex 3-D geometry of the drill has been developed by using CAD software. The drill has a point angle of 135°, helix angle of 30°, and diameter of 6.35 mm. Each drill cutting edge is split into seven segments of the elementary cutting tools (ECT). The drill CAD model is exported in ABAQUS™ for mesh generation and thermal analysis. The finite element mesh of the drill, which contains 84,142 four-node tetrahedral elements with heat transfer elements of type DC3D4 has been used for the analysis of

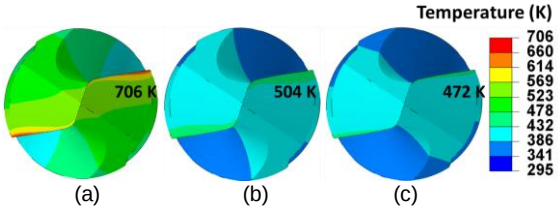

Fig. 2(a-c): Variation of temperature at cutting speed of 10 m/min under (a) Dry condition (b) Heat sink bottom channel cooling (c) Ti+Cu scheme, after 6.35 mm depth of drilling

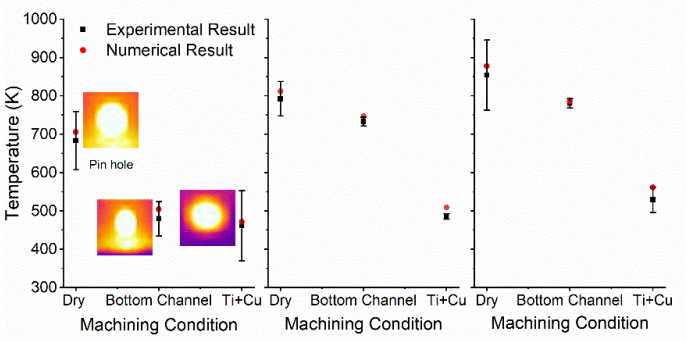

Fig. 3(a-c): Comparison of numerical and present experimental results for maximum temperature after 6.35 mm depth of drilling for different cutting speeds. (a) 10 m/min, (b) 25 m/min, (c) 35 m/min cutting speeds with a feed rate of 0.051 mm/rev under various cutting environments.

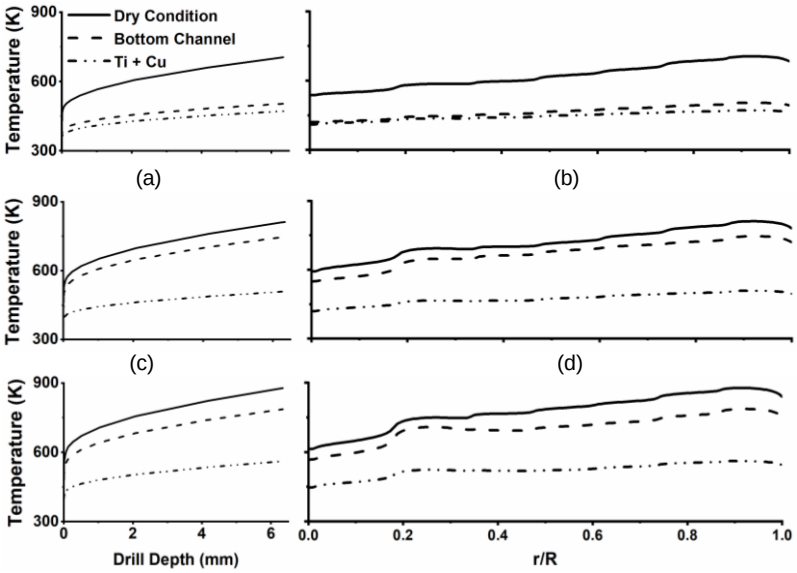

Fig. **4(**a-f): (a, c, e) Temporal and (b, d, f) Spatial distribution of temperature along the cutting edge on various cutting environments at (a,b) 10 m/min, (c,d) 25 m/min and (e,f) 35 m/min cutting speeds

temperature distribution. A constant heat flux was applied on each ECT over the area of tool-chip contact, as shown in Fig. 1d.

4. Results and discussions

4.1 Temperature Distribution and Validation of Measured Drill Temperature

The finite element method was used to predict the temperature distribution for drilling of titanium alloys under different cutting environments. Fig. 2a-c shows spatial distribution of temperature on a drill after 6.35 mm depth of drilling for cutting speed of 10 m/min and under different cooling environments. A close observation shows that a higher temperature occurs in the region near to the end of tool cutting edge. The maximum temperature of the drill reduces with the new cutting environments. The decrease of temperature was due to fluid flow in the bottom channel cooling that carried away the heat generated in the cutting zones through convection. In case of Ti-Cu condition, the maximum temperature reduced due to higher thermal conductivity of the adjacent copper plate. Similarly, the temperature distribution was also observed as the cutting speed changes from 25 and 35 m/min under various cutting environments. The maximum temperature of the drill reduced by 8-30 % and 32-38 % by using bottom channel and Ti-Cu scheme, respectively in comparison to the dry condition. The experimental results were compared with the predicted temperature using numerical analysis under various cutting environments shown in Fig. 3a-c. The predicted temperatures lie within an error of ~1-6 %, of average experimental temperature.

4.2 Spatial and Temporal Variation of Temperature on Drill

The temporal distribution of the drilling temperature during the drilling of 6.35 mm hole in workpiece is shown in Figs. 4(a,c,e). As the drill engages with the workpiece, the temperature increases suddenly. The drill temperature continues to increase as the drill moves deep into the workpiece due to the accumulation of heat in different cutting zones. Figs. 4b-d-f show the spatial distribution of drill temperature while drilling 6.35 mm hole in a plate of titanium. The spatial temperature profiles are generated along the cutting edge as a function of r/R, where, r varies at a point on cutting edge with respect to center of drill, and R is the maximum drill radius. It observed that as r/R increases, the temperature increases gradually, see Fig 4b. This is because, r/R=1 represents drill corner,

where the peripheral cutting speed is maximum. Also, with different cooling conditions, temperature obtained is lower than the dry cutting condition. This is due to introduction of higher thermal conductivity of copper in Ti-Cu combination and bottom channel cooling that carries away the heat generated in the cutting zones through convection. An increase of cutting speed, however increases the temperature due to the higher rate of heat generation.

4.3 Experimental Thrust and Torque

Thrust and torque gradually increase until the drill cutting edge is fully engaged within the workpiece. When drill cutting edges encounter the pin-hole of ϕ 2 mm in the workpiece, a drop in the thrust and torque is recorded. The average thrust and torque during the full engagement of the cutting edge under various cutting environments are plotted in Figure 5a-b. The average thrust on the drill is reduced by 3 to 17 % and 8 to17 % in the bottom channel and Ti-Cu scheme, respectively, in comparison to the dry condition. The maximum average torque on the drill is reduced by 9 to 15 % and 10 to 20 % in the bottom channel and Ti-Cu combination, respectively, with respect to the dry condition.

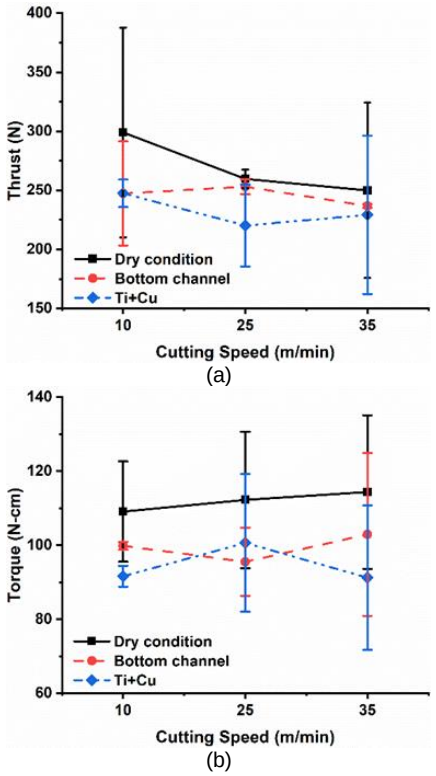

Fig. 5(a-b): Average (a) Thrust and (b) Torque variation under different cutting environments

5. Conclusions

New cooling techniques to improve heat dissipation in drilling of titanium alloy, such as Ti-Cu butt joint and heat-sink based bottom channel cooling, have been proposed. The introduction of higher thermal conductivity of copper in the Ti-Cu combination and the flow of water in a heat sink in the bottom channel can effectively carry away the generated heat from the cutting zones. We have used a finite element model to evaluate temperature distribution and maximum temperature in a drill.

The numerical results show that the maximum temperature of drill was reduced by 8 to 30% and 32 to 38% in the bottom channel and Ti-Cu scheme, respectively, in comparison to the dry condition. The numerical temperatures lie within ~1-6% of the experimental values.

The Ti-Cu butt joint performed well in terms of reduction in maximum temperature, thrust forces and torque in comparison with heat sink bottom channel cooling.

Acknowledgements

We would like to thank the partial financial support from the National Centre for Aerospace Innovation and Research (NCAIR), IIT Bombay, Mumbai.

References

[1] E. O. Ezugwu et al., “An overview of the machinability of aeroengine alloys,” J. Mater. Process. Technol., vol.134, no.2, pp. 233–253, 2003.
[2] M. B. Da Silva et al., “Cutting temperature: prediction and measurement methods - a review” J. Mater. Process. Technol., vol.88, no.1, pp.195–202, 1999.
[3] L. S. Ahmed et al., “Cryogenic Drilling of Ti-6Al-4V Alloy Under Liquid Nitrogen Cooling” Mater. Manuf. Process., vol.31, no.7, pp. 951–959, 2016.
[4] A. Suarez et al., “Effects of High-Pressure Cooling on the Wear Patterns on Turning Inserts Used on Alloy IN718” Mater. Manuf. Process., 2016.
[5] S. A. Chowdhury et al., “Effectiveness of Using CFD for Comparing Tool Cooling Methods” Lect. Notes Eng. Comput. Sci., vol.2, pp. 1076–1081, 2014.
[6] C. Tahri, et al., “CFD Simulation and Optimize of LN_2 Flow Inside Channels Used for Cryogenic Machining: Application to Milling of Titanium Alloy Ti-6Al-4V” Procedia CIRP, vol. 58, pp. 584–589, 2017.
[7] S. Pervaiz et al., “A Coupled FE and CFD Approach to Predict the Cutting Tool Temperature Profile in Machining” Procedia CIRP, vol. 17, pp. 750–754, 2014.
[8] H. S. Patne et al., “Modeling of temperature distribution in drilling of titanium” Int. J. Mech. Sci., vol. 133, pp. 598–610, 2017.
[9] E. M. Berliner et al., “Analytic calculations of the temperature field and heat flows on the tool surface in metal cutting due to sliding friction” Wear, vol.143, no.2, pp. 379–395, 1991.
[10] P. L. B. Oxley, “Mechanics of metal cutting,” Int. J. Mach. Tool Des. Res., vol. 1, no. 1, pp. 89–97, 1961.
[11] R. Li et al., “Tool temperature in titanium drilling” J. Manuf. Sci. Eng. Trans. ASME, vol. 129, no. 4, pp. 740–749, 2007.
[12] Y. Huang et al., “Modelling of the cutting temperature distribution under the tool flank wear effect” Proc. Inst. Mech. Eng. Part C-journal Mech. Eng. Sci. - proc inst mech eng c-j mech e, vol. 217, pp. 1195–1208, 2003.
[13] A. Fatima et al., “A review of tool-chip contact length models in machining and future direction for improvement” Proc. Inst. Mech. Eng. Part B J. Eng. Manuf., vol. 227, no. 3, pp. 345–356, 2013.
[14] J. P. Holman, Heat Transfer, 10th ed. New York: McGraw Hill Higher Education, 2010.